HIP-2003-19/TH
ROME1-1352/2003

Large extra dimension effects in Higgs boson production at linear colliders and Higgs factories

Anindya Datta[1], Emidio Gabrielli[1], and Barbara Mele[2]

[1] *Helsinki Institute of Physics, POB 64, University of Helsinki, FIN 00014, Finland*
[2] *Istituto Nazionale di Fisica Nucleare, Sezione di Roma, and Dip. di Fisica, Università La Sapienza, P.le A. Moro 2, I-00185 Rome, Italy*

Abstract

In the framework of quantum gravity propagating in large extra dimensions, the effects of virtual Kaluza-Klein graviton and graviscalar interference with Higgs boson production amplitudes are computed at linear colliders and Higgs factories. The interference of the almost-continuous spectrum of the KK gravitons with the standard model *resonant* amplitude is finite and predictable in terms of the fundamental D-dimensional Plank scale M_D and the number of extra dimensions δ. We find that, for $M_D \simeq 1$ TeV and $\delta = 2$, effects of the order of a few percent could be detected for heavy Higgs bosons ($m_H > 500$ GeV) in Higgs production both via WW fusion in e^+e^- colliders and at $\mu^+\mu^-$ Higgs-boson factories.

1 Introduction

In recent years much attention has been paied to theories where the weakness of the gravitational coupling is explained by the presence of *large* compact extra spatial dimensions, as shown in [1]. In such theories, while standard model (SM) fields are confined in the usual 4-dimensional space, the gravity can propagate in the full high dimensional space, and its intensity is diluted in the large volume of the extra dimensions.

The Newton's constant G_N in the 3+1 dimensional space is then related to the corresponding Planck scale M_D in the $D = 4 + \delta$ dimensional space by

$$G_N^{-1} = 8\pi R^\delta M_D^{2+\delta} \tag{1}$$

where R is the radius of a compact manifold assumed to be on a torus. According to the present limits on Newton's law [2], one could have $M_D \sim 1$ TeV if the number of extra dimensions is $\delta \geq 2$.

A crucial consequence of this framework is that quantum gravity effects could become strong at the TeV scale and measurable at future high-energy colliders. After integrating out the compact extra dimensions, the effective Einstein theory in 3+1 dimensions reliably describes the interactions of the extra-dimensional gravitons with gauge and matter fields [3, 4, 5]. An essentially continuum spectrum of massive Kaluza-Klein (KK) excitations of the standard graviton field arises, for δ not larger than about 6. When summing over the allowed spectrum of KK states either in the inclusive production or in the exchange of virtual KK gravitons, the small coupling $(E/M_P)^2$ associated to a single graviton production/exchange (where E is the typical energy of the process and M_P is the Plank mass) is replaced by the quantity $(E/M_D)^{2+\delta}$. Then, for $M_D \sim 1$ TeV, processes involving gravitons could well be detected at present and future high-energy colliders. This possibility has been quite thoroughly explored in a number of papers [3]-[8].

Regarding processes with virtual KK graviton exchange, it is well known that in general the corresponding amplitude is divergent and not computable in the effective theory [3]. In particular, the *real* part of the amplitude, $Re[\mathcal{A}]$, needs an ultraviolet cut-off. This means that in general the theory is not predictive in the sector of virtual KK graviton exchange. On the other hand, the *imaginary* part of the amplitude, $Im[\mathcal{A}]$, is finite and cutoff independent, being connected to the branch-cut singularity of real graviton emission [3]. In a recent paper [8], we stressed that this can have important consequences, when considering standard model (SM) *resonant* processes interfering with virtual KK graviton exchange graphs. In fact, the corresponding interference, that is dominated by $Im[\mathcal{A}]$, turns out to be *finite*, and predictable in terms of the fundamental Plank scale M_D and the number of extra dimensions δ.

In [8], we applied this observation to LEP physics, and computed the effects on the $e^+e^- \to f\bar{f}$ physical observables of the interference of the virtual KK graviton-exchange amplitude with the resonant SM amplitude at the Z boson pole. We found that, although the corresponding impact on total cross-sections vanishes, there are finite modifications of different asymmetries, whose relative effect amounts, in the most favorable cases, to about 10^{-4}.

In the present paper, we want to extend this approach to the case of a heavy Higgs boson (H) production at future linear e^+e^- colliders and $\mu\mu$ colliders. By *heavy*, we will imply $m_H \geq 200$ GeV. Graviton interference effects on cross-sections turns out to be proportional to the ratio of the total width over the mass of the resonance state, due to the imaginary part of the SM amplitude [8]. Then, one expects to find remarkably more conspicuous graviton interference effects in a heavy Higgs boson production than in the Z^0 boson pole physics, due to the rapidly growing Higgs width with the Higgs mass. One can compare , e.g., $\Gamma_Z/M_Z \simeq 0.027$ with $\Gamma_H/m_H \simeq 0.072, 0.29$ for $m_H = 400, 700$ GeV, respectively. Moreover, the imaginary part of the graviton amplitude grows quite rapidly with the process c.o.m. energy.

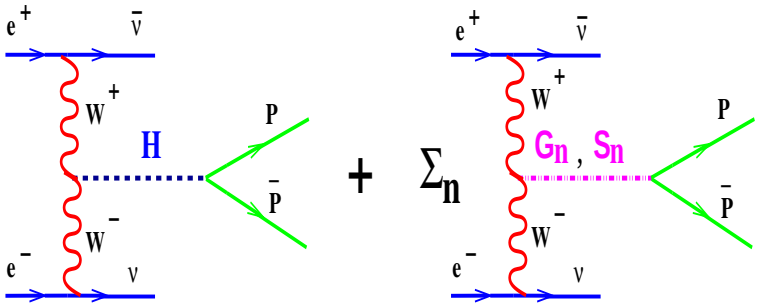

Figure 1: *Feynman diagrams of the processes in Eq. (2).*

At linear e^+e^- colliders [9], we consider the Higgs production via vector boson fusion with the subsequent H decay into pairs of heavy particles

$$e^+e^-(WW) \to \nu\bar{\nu}H \to \nu\bar{\nu}WW,\ \nu\bar{\nu}ZZ,\ \nu\bar{\nu}t\bar{t}\,. \tag{2}$$

Feynman diagrams for these processes are presented in Figure 1. This process is one of the dominant H production mechanism at linear colliders, and becomes the main one at $\sqrt{S} \geq 500$ GeV [10]. The same initial and final states can be mediated by a continuous spectrum of KK spin-2 gravitons, G_n, and spin-0 graviscalars, S_n, in the s channel *

$$\sum_n \left\{e^+e^-(WW) \to \nu\bar{\nu}\,G_n^*,\ \nu\bar{\nu}\,S_n^* \to \nu\bar{\nu}WW,\ \nu\bar{\nu}ZZ,\ \nu\bar{\nu}t\bar{t}\right\}\,. \tag{3}$$

These processes at energies $\sqrt{S} \gg M_W$ can be reliably treated in the effective-W approximations [11], by convoluting the cross-sections for the subprocesses

$$WW \to H \to WW, ZZ, t\bar{t}\,, \tag{4}$$

*We neglect here possible t channel amplitudes, that give subdominant contributions in the following.

and

$$\sum_n \{WW \to G_n^*,\ S_n^* \to WW, ZZ, t\bar{t}\} \tag{5}$$

with the appropriate W distributions in the electron beam (same for ZZ initiated processes).

On the Higgs boson resonance, the interference of the processes eqs.(4) and (5) will be dominated by the imaginary part of the graviton/graviscalar amplitude, that, as discussed above, is finite and predictable in terms of M_D and δ.

The aim of the present paper is to determine the amount by which the Higgs production cross-sections and distributions can be affected by the interference with the KK graviton/graviscalar amplitude. We then discuss the possibility to measure such an effect (and, hence, to find a footprint of a large extra dimension theory) at realistic linear collider machines.

In the last part of the paper we also analyze KK graviton/graviscalar interference effects in Higgs production at a possible $\mu\mu$ collider acting as a Higgs boson factory [12], through the channels

$$\mu^+\mu^- \to H \to WW, ZZ, t\bar{t}\,, \tag{6}$$

and

$$\sum_n \left\{\mu^+\mu^- \to G_n^*,\ S_n^* \to WW, ZZ, t\bar{t}\right\}\ . \tag{7}$$

This process would presumably be affected by smaller theoretical uncertainty, and could provide an even more sensitive probe to large extra dimension effects.

2 The virtual-graviton exchange amplitude

We are interested in computing the interference of the exchange of a virtual KK spin-2 graviton and a virtual KK spin-0 graviscalar with a resonant SM scattering amplitude. Hence, we will analyze in particular an s-channel KK exchange amplitude. We will follow in this section the approach of [3].

The graviton-mediated scattering amplitude in the momentum space is obtained by summing over all KK modes

$$\mathcal{A} = \frac{1}{\bar{M}_P^2} \sum_n \left\{ T_{\mu\nu} \frac{P^{\mu\nu\alpha\beta}}{s - m_n^2} T_{\alpha\beta} + \frac{1}{3} \left(\frac{\delta - 1}{\delta + 2} \right) \frac{T_\mu^\mu T_\nu^\nu}{s - m_n^2} \right\}\ , \tag{8}$$

where $\bar{M}_P$ is the reduced Plank mass ($\bar{M}_P = M_P/\sqrt{8\pi}$), and $T_{\mu\nu}$ is the energy-momentum tensor of the scattering fields. The first and second terms in Eq. (8) corresponds to graviton and graviscalar exchanges respectively (here m_n represents

both the graviton and graviscalar masses without loss of any generality). In the unitary gauge, the projector of the graviton propagator, $P^{\mu\nu\alpha\beta}$, is given by

$$P^{\mu\nu\alpha\beta} = \frac{1}{2}\left(\eta^{\mu\alpha}\eta^{\nu\beta} + \eta^{\mu\beta}\eta^{\nu\alpha}\right) - \frac{1}{3}\eta^{\mu\nu}\eta^{\alpha\beta} + \dots \tag{9}$$

where $\eta^{\mu\nu}$ is the Minkowski metric. Dots represent terms proportional to the graviton momentum q_μ, that, being $q^\mu T_{\mu\nu} = 0$, give a vanishing contribution to the amplitude. The trace of $T_{\mu\nu}$ is nonvanishing only for massive initial and final states.

Since the energy-momentum tensors do not depend on KK indices, one can perform the sum (over n) irrespective of the scattering process, and Eq. (8) becomes

$$\mathcal{A} = \mathcal{S}(s)\mathcal{T}, \quad \mathcal{S}(s) = \frac{1}{\bar{M}_P^2}\sum_n \frac{1}{s - m_n^2}, \quad \mathcal{T} = T_{\mu\nu}T^{\mu\nu} - \frac{1}{\delta+2}T^\mu_\mu T^\nu_\nu \tag{10}$$

In the continuum approximation for the KK graviton spectrum, one then obtains

$$\mathcal{S}(s) = \frac{1}{M_D^{2+\delta}}\int d^\delta q_T \frac{1}{s - q_T^2} = \frac{\pi^{\frac{\delta}{2}}}{M_D^4}\Gamma(1-\frac{\delta}{2})\left(-\frac{s}{M_D^2}\right)^{\frac{\delta}{2}-1} \tag{11}$$

where we assumed $m_n^2 = q_T^2$, with q_T the graviton momentum orthogonal to the brane.

In the interference with a resonant amplitude, only $Im[\mathcal{S}(s)]$ will contribute, with

$$Im[\mathcal{S}(s)] = -\frac{\pi}{M_D^{2+\delta}}\frac{S_{\delta-1}}{2}s^{\frac{\delta-2}{2}} \tag{12}$$

where $S_{\delta-1}$ is the area of the δ sphere. For $\delta = 2n$, $S_{\delta-1} = 2\pi^n/(n-1)!$ and, for $\delta = 2n+1$, $S_{\delta-1} = 2\pi^n/\prod_{k=0}^{n-1}(k+\frac{1}{2})$, with n integer. Hence, imaginary part of the amplitude is finite and predictable, only depending on the D-dimensional Plank scale M_D and on the number of extra dimensions δ. It also grows quite rapidly with $\sqrt{s}$ for $\delta > 2$.

On the other hand, as discussed in the previous section, divergences in general arise in the real part of $\mathcal{S}$. They can be regularized by introducing an external cut off that spoils the predictivity of the theory, parametrizing unknown new-physics contributions in the ultraviolet region. This feature makes virtual graviton exchange processes phenomenologically less interesting than the real graviton production processes, unless the imaginary part of the amplitude can be separated. This is exactly what happens when considering the graviton interferences with resonant SM scattering amplitudes. The latter case is indeed the subject of our previous work in [8] and of the present paper.

3 Interference effects in the WW partonic cross-sections

In this section, we determine the effects on the angular distributions and cross-sections of the WW fusion Higgs production processes in Eq. (2) arising from their interferences with the corresponding KK graviton/graviscalar exchange processes in Eq. (3). We start from the *partonic* WW initiated amplitude for the processes

$$WW \to H \to WW, ZZ, t\bar{t}\,, \tag{13}$$

and

$$\sum_n \{WW \to G_n^*,\ S_n^* \to WW, ZZ, t\bar{t}\}\ , \tag{14}$$

we compute their interferences, and then convolute them (along with the corresponding SM cross sections as in Eq. (13) with the effective-W distributions in the initial electron/positron beams.

We notice that due to the different spin properties of the Higgs ($s = 0$), graviton ($s = 2$) and graviscalar ($s = 0$) intermediate states, only the graviton will have a nontrivial impact on the angular distribution. On the other hand, the latter effect will vanish in the total cross section, since different spin amplitudes turn out to be orthogonal. An analogous effect can be observed in the Z boson - graviton interference in [8].

The initial W polarizations that are relevant for Higgs production are the ones where both the W's are either transverse (with opposite polarization projection) or longitudinal. We call the two combinations, $\lambda = T$ and $\lambda = L$, respectively.

If P stands for one of the possible final particles W, Z and t in Eq. (13), the polarization dependent angular distribution for the process $W^+W^- \to P\bar{P}$ via Higgs exchange plus interference effects with the graviton/graviscalar mediated scattering reads, near the Higgs boson pole (i.e., for $|\sqrt{\hat{s}} - m_H| < \Gamma_H$) [†] is given by

$$\frac{d\sigma_\lambda^P}{d\cos\theta} \;=\; \frac{\bar{\sigma}_\lambda^P}{2}\,\left\{1 + \Delta_0^P + \Delta_{2,\lambda}^P\,(1 - 3\cos^2\theta)\right\}\ , \tag{15}$$

where θ is the polar angle of one of the final particle with respect to the beam in the c.o.m. frame. Nonvanishing coefficients Δ_0^P and $\Delta_{2,\lambda}^P$ arise from the interference of the Higgs exchange amplitude with the graviscalar and graviton exchange amplitudes, respectively. In particular, a nonvanishing graviton contribution alters the $\cos\theta$ independent distribution predicted by the SM Higgs exchange. $\bar{\sigma}_\lambda^P$ stands for the SM

[†] Contributions coming from the real part of the amplitudes are suppressed by terms of order $|\hat{s} - m_H^2|/m_H^2$ in this case.

Higgs-exchange total cross section for the process $W^+W^- \to P\bar{P}$,

$$\bar{\sigma}_\lambda^P = \frac{1}{16\pi\hat{s}} \, \frac{g^4 m_W^4 \xi_P}{(\hat{s}-m_H^2)^2 + m_H^2\Gamma_H^2} \, \sqrt{\frac{\hat{s}-4m_P^2}{\hat{s}-4m_W^2}} \, \rho_\lambda^P\left(\frac{\hat{s}}{m_W^2}\right). \tag{16}$$

In the last equation, g is the electroweak $SU(2)$ coupling, m_P, m_W, and m_H stand for the P, W, and H masses, respectively, Γ_H is the total Higgs width, $\sqrt{\hat{s}}$ is the total energy of the initial W's in their c.o.m. frame, and ξ_P are numerical coefficients ($\xi_t = \xi_W = 1$, and $\xi_Z = \frac{1}{2}$). The functions $\rho_\lambda^P(x)$ are given by

$$\begin{aligned}
\rho_L^t(x) &= \frac{(x-2)^2}{4}\rho_T^t(x) \;, \quad \rho_T^t(x) = \frac{3}{2} r_t (x - 4r_t) \\
\rho_L^V(x) &= \frac{(x-2)^2}{4}\rho_T^V(x) \;, \quad \rho_T^V(x) = \frac{(x^2 - 4x r_V + 12 r_V^2)}{4}
\end{aligned}$$

where, $V = (W, Z)$, $r_t = m_t^2/m_W^2$, $r_W = 1$, and $r_Z = m_Z^2/m_W^2$.

Finally, we present the expressions of the coefficients Δ_0^P and $\Delta_{2,\lambda}^P$ in Eq. (15), arising from the interference of the SM Higgs exchange amplitude near the Higgs pole with the imaginary part [cf. Eq. (12)] of the graviscalar/graviton exchange amplitude

$$\begin{aligned}
\Delta_0^P &= R_\delta \, c_P \left(\frac{\delta - 1}{\delta + 2}\right) \;, \quad \Delta_{2,\lambda}^P = R_\delta \, f_\lambda^P \left(\frac{\hat{s}}{m_W^2}\right) \\
R_\delta &= \frac{S_{\delta-1}\pi}{4\sqrt{2} G_F M_D^2} \left(\frac{\sqrt{\hat{s}}}{M_D}\right)^\delta \left(\frac{m_H \Gamma_H}{\hat{s}}\right)
\end{aligned} \tag{17}$$

where c_P are numerical coefficients ($c_W = \frac{4}{3}$, $c_Z = \frac{2}{3}$, and $c_t = \frac{4}{3}$), and the functions $f_\lambda^P(x)$s are defined as

$$\begin{aligned}
f_L^t(x) &= -\frac{1}{2}\left(\frac{x+4}{x-2}\right) f_T^t(x) \;, \quad f_T^t(x) = -\frac{4}{3} \\
f_L^V(x) &= -\frac{1}{2}\left(\frac{x+4}{x-2}\right) f_T^V(x) \;, \quad f_T^V(x) = \frac{2}{3}\frac{(x-4r_V)(x+6r_V)}{(x^2 - 4x r_V + 12 r_V^2)} \,.
\end{aligned} \tag{18}$$

We recall that interference effects arising from the *real* part of the amplitudes (that we are neglecting) are suppressed by terms of order $|\hat{s} - m_H^2|/m_H^2$ on the Breit-Wigner resonance.

When convoluting the *partonic* WW cross sections with the W's effective fluxes in the collider beams, it will be useful to approximate the Breit-Wigner propagator in Eq. (16) by a Dirac delta function

$$\frac{1}{(\hat{s}-m_H^2)^2 + m_H^2\Gamma_H^2} \longrightarrow \frac{\pi}{m_H \Gamma_H} \, \delta(\hat{s} - m_H^2) \,. \tag{19}$$

A few basic features of the distribution in Eq. (15) can be discussed even before making the convolution with the W's fluxes. First of all, as anticipated, the spin structure of the intermediate states determine a flat (Higgs-like) angular distribution for the graviscalar interference contribution, affecting the total cross section by an amount $\Delta_0^P \times \sigma_{SM}$. On the other hand, the spin-2 gravitons give rise to a $(1-3\cos^2\theta)$ angular distribution in the WW c.o.m frame, that gives a vanishing result on the total cross section. Nevertheless, an angular analysis of the final state will reflect the nontrivial impact of the $(1-3\cos^2\theta)$ distribution in the WW c.o.m system on the laboratory-frame angular characteristics. For instance, some angular cut on the directions of the final states P with respect to the electron/positron beams will originate a non null effect (weighted by the coefficients $\Delta_{2,L}^P$ and $\Delta_{2,T}^P$) in the integrated cross sections.

In order to establish the general relevance of the present effects, it is of course crucial to analyze the numerical values of the coefficients Δ_0^P and $\Delta_{2,\lambda}^P$ for interesting cases of the model parameters. In Tables 1 and 2 the most favorable (experimentally allowed) case of $M_D = 1$ TeV with $\delta = 2$ is presented for the processes $W^+W^- \to W^+W^-$ and $W^+W^- \to t\bar{t}$, respectively. The coefficients Δ_0^P and $\Delta_{2,\lambda}^P$ have been evaluated at $\sqrt{\hat{s}} = m_H$, and are presented for different Higgs masses (with $m_H \leq 800$ GeV) and corresponding total widths. The values of relevant SM parameters in the computation are set as in [13]. The case $W^+W^- \to ZZ$ can be easily inferred from Table 1, since $\Delta_0^Z = \Delta_0^W/2$ and, apart from $o(M_Z^2/M_W^2 - 1)$ effects, $\Delta_{2,\lambda}^Z = \Delta_{2,\lambda}^W$.

$m_H(GeV)$	$\Gamma_H(GeV)$	$\Delta_{2,T}^W$	$\Delta_{2,L}^W$	Δ_0^W
200	1.4	5.9×10^{-5}	-7.1×10^{-5}	2.8×10^{-5}
300	8.5	6.7×10^{-4}	-5.1×10^{-4}	2.6×10^{-4}
400	29.	2.8×10^{-3}	-1.7×10^{-3}	1.1×10^{-3}
500	67.	7.7×10^{-3}	-4.4×10^{-3}	3.3×10^{-3}
600	123.	1.6×10^{-2}	-9.0×10^{-3}	7.3×10^{-3}
700	200.	3.0×10^{-2}	-1.6×10^{-2}	1.4×10^{-2}
800	309.	5.2×10^{-2}	-2.7×10^{-2}	2.4×10^{-2}

Table 1: Numerical values of $\Delta_{2,T}$, $\Delta_{2,L}$ and Δ_0 for various Higgs masses if $\delta = 2$ and $M_D = 1$ TeV, for the process $W^+W^- \to W^+W^-$.

The leading dependence on the Higgs mass of the coefficients Δ_0^P and $\Delta_{2,\lambda}^P$ arises from the R_δ behavior as a function of m_H and Γ_H. In general, from Eq. (17), on the

$m_H(GeV)$	$\Gamma_H(GeV)$	$\Delta^t_{2,T}$	$\Delta^t_{2,L}$	Δ^t_0
400	29.	-4.5×10^{-3}	2.7×10^{-3}	1.1×10^{-3}
500	67.	-1.3×10^{-2}	7.8×10^{-3}	3.3×10^{-3}
600	123.	-2.7×10^{-2}	1.6×10^{-2}	7.3×10^{-3}
700	200.	-5.6×10^{-2}	3.0×10^{-2}	1.4×10^{-2}
800	309.	-9.7×10^{-2}	5.0×10^{-2}	2.4×10^{-2}

Table 2: Numerical values of $\Delta_{2,T}$, $\Delta_{2,L}$ and Δ_0 for various Higgs masses if $\delta = 2$ and $M_D = 1$ TeV, for the process $W^+W^- \to t\bar{t}$.

Higgs peak, one has

$$R_\delta \sim \frac{S_{\delta-1}}{G_F M_D^2} \left(\frac{m_H}{M_D}\right)^\delta \left(\frac{\Gamma_H}{m_H}\right) . \tag{20}$$

At $\delta = 2$, $R_2 \sim m_H \Gamma_H$, and this largely explains the increase of Δ^P_0 and $\Delta^P_{2,\lambda}$ with m_H observed in Tables 1 and 2. One can note that for $m_H > 500$ GeV most of the coefficients are quite large, and could have an impact on the measurable cross-sections. At $m_H = 800$ GeV, all the coefficients amount to a few percent. The most striking one seems to be the graviton-interference case in the top quark channel, that gives $\Delta^t_{2,T} \simeq -0.1$ at $m_H \simeq 800$ GeV.

On the other hand, increasing the Planck scale M_D can quite affect the coefficient values considered above. From Eq. (20), one has $R_\delta \sim 1/M_D^{2+\delta}$. Increasing M_D by a factor 2 would imply, for instance, a reduction by a factor about 1/16 on the coefficients values shown in Tables 1 and 2.

4 Interference effects in the e^+e^- cross-sections

In the previous section, we have shown that, after integrating over the full range of $\cos\theta$ the $W^+W^- \to P\bar{P}$ angular distribution, the *graviton* interference, weighted by the function $(1 - 3\cos^2\theta)$, vanishes. Only *graviscalar*-interference effects survive, affecting the total cross sections by a factor $(1 + \Delta^P_0)$. The latter will modify the corresponding total cross-sections in e^+e^- collisions. In order to pin down the *graviton*-interference coefficients $\Delta^P_{2,\lambda}$, one should instead optimize the angular analysis of the process by defining proper strategies (like angular cuts or new asymmetries) that can enhance the graviton contribution (cf. [8]). To this end, it is crucial to consider the laboratory-frame angular distribution for the complete process $e^+e^-(WW) \to \nu\bar{\nu}P\bar{P}$, that can be obtained by properly boosting the subprocess $W^+W^- \to P\bar{P}$ according to the initial WW fluxes in the electron/positron beams.

In a laboratory frame where the initial WW systems moves with velocity β, the $W^+W^- \to P\bar{P}$ angular distribution in Eq. (15) becomes

$$\frac{d\sigma^P_\lambda}{d\cos\theta_L} = \frac{\bar{\sigma}^P_\lambda}{2}\left[1+\Delta^P_0+\Delta^P_{2,\lambda}\,\mathcal{F}(\theta_L,\beta)\right]\,\mathcal{J}(\theta_L,\beta)\,, \tag{21}$$

where

$$\mathcal{F}(\theta_L,\beta)\equiv 1-3\left(\frac{\cos\theta_L-\beta}{1-\cos\theta_L\beta}\right)^2;\qquad \mathcal{J}(\theta_L,\beta)\equiv\frac{1-\beta^2}{(1-\beta\cos\theta_L)^2}\,, \tag{22}$$

and θ_L is the P scattering angle in laboratory frame. Above, we have neglected terms of order m^2_W/E^2_e.

We then fold the above *partonic* cross sections with the probabilities $P^W_\lambda(x)$ of emitting from an $e^+(e^-)$ beam a real W with polarization λ and fraction of the beam momentum x. The $e^+e^-(WW)\to\nu\bar{\nu}P\bar{P}$ differential cross-section can be written as

$$\frac{d\sigma^P_{ee}(S)}{d\cos\theta_L}=\Sigma_{\lambda=L,T}\int dx_1\,dx_2\,\left\{P^W_\lambda(x_1)\,P^W_\lambda(x_2)\,\frac{d\sigma^P_\lambda(\hat{s})}{d\cos\theta_L}\right\} \tag{23}$$

where $\hat{s}=x_1x_2S$ and $\sqrt{S}=2E_e$, with E_e the energy of the beam in the laboratory c.o.m. system. For the W-fluxes, we assume the expressions [11]

$$\begin{aligned} P^W_T(x) &= \frac{g^2}{64\pi^2}\,\frac{x^2+2(1-x)}{x}\log\left(\frac{S}{m^2_W}\right)\\ P^W_L(x) &= \frac{g^2}{32\pi^2}\,\left(\frac{1-x}{x}\right)\,. \end{aligned} \tag{24}$$

We now can have the laboratory-frame angular distribution for the complete process $e^+e^-(WW)\to\nu\bar{\nu}P\bar{P}$, by convoluting Eq. (21) with the W-fluxes. By introducing the variables

$$\tau=\frac{m^2_H}{S},\qquad \beta=\frac{x^2-\tau}{x^2+\tau},\qquad r_H=\frac{m^2_H}{m^2_W}\,, \tag{25}$$

and the definition

$$N_P=\frac{g^4m^4_W\xi_P}{32Sm^3_H\Gamma_h}\,\sqrt{\frac{r_H-4r_P}{r_H-4}}\,\rho^P_T(r_H)\,, \tag{26}$$

and, by making use of Eq. (19), one has from Eqs. (21) and (23)

$$\frac{d\sigma^P_{ee}}{d\cos\theta_L} = N_P\left\{(1+\Delta^P_0)\,\left[I^L_0(\theta_L)+I^T_0(\theta_L)\right]+\Delta^P_{2,L}\,I^L_2(\theta_L)+\Delta^P_{2,T}\,I^T_2(\theta_L)\right\} \tag{27}$$

where the functions $I^\lambda_{0,2}(\theta_L)$ include the integration of the W distributions. In particular,

$$I^T_0(\theta_L) = 2\int_\tau^1\frac{dx}{x}\,P^W_T(x)P^W_T\left(\frac{\tau}{x}\right)\,\mathcal{J}(\theta_L,\beta) \tag{28}$$

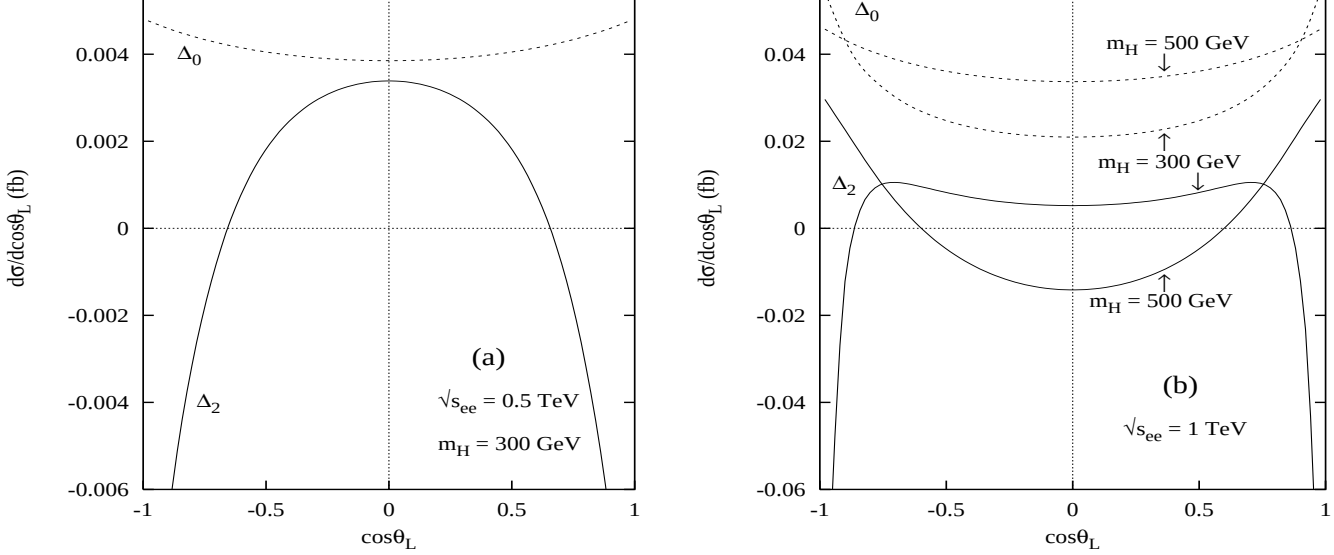

Figure 2: *Graviton (solid line) and graviscalar (dashed line) contributions to the angular distribution in the laboratory frame [Eq. (27)] for e^+e^- center-of-mass energies (a) 500 GeV and (b) 1 TeV.*

$$I_0^L(\theta_L) = \frac{(r_H-2)^2}{4}\int_\tau^1 \frac{dx}{x}\, P_L^W(x) P_L^W\left(\frac{\tau}{x}\right)\, \mathcal{J}(\theta_L,\beta) \tag{29}$$

$$I_2^T(\theta_L) = 2\int_\tau^1 \frac{dx}{x}\, P_T^W(x) P_T^W\left(\frac{\tau}{x}\right)\, \mathcal{J}(\theta_L,\beta)\, \mathcal{F}(\theta_L,\beta) \tag{30}$$

$$I_2^L(\theta_L) = \frac{(r_H-2)^2}{4}\int_\tau^1 \frac{dx}{x}\, P_L^W(x) P_L^W\left(\frac{\tau}{x}\right)\, \mathcal{J}(\theta_L,\beta)\, \mathcal{F}(\theta_L,\beta)\,, \tag{31}$$

where the factor 2 in the transverse functions $I_{0,2}^T(\theta_L)$ comes from the two different initial W polarization transverse projections that contribute to a spin-0 state.

For the graviton component, the zeros of the $(1-3\cos^2\theta)$ distribution in the WW c.o.m. frame are in general shifted by the WW boosts to higher values of $|\cos\theta|$.

In Figure 2a, we show (by the symbol Δ_0) the graviscalar contribution and (by the symbol Δ_2) the graviton contribution (including both the longitudinal and the transverse part) to the total interference with the SM amplitude in the angular distribution in Eq. (27), at $\sqrt{S} = 500$ GeV and $m_H = 300$ GeV.

In order to pin down the *graviton* contribution in Eq. (27), one can then measure the angular distribution integrated over a selected $\cos\theta_L$ range, where the corresponding distribution keeps, for instance, a positive (or a negative) value. The corresponding cross section measured with an angular cut $|\cos\theta_L| < \epsilon$ (where $\pm\epsilon$ could be the zeros of the distribution) will be given by

$$\sigma_{ee}^{P,\epsilon} = \bar{\sigma}_{ee}^{P,\epsilon}\, \left(1 + \Delta_0^P + \alpha_L^\epsilon \Delta_{2,L}^P + \alpha_T^\epsilon \Delta_{2,T}^P\right)\,, \tag{32}$$

with

$$\bar{\sigma}_{ee}^{P,\epsilon} = N_P \int_{-\epsilon}^{\epsilon} d\cos\theta_L\, \left[I_0^L(\theta_L) + I_0^T(\theta_L)\right]\,,$$

$$\alpha_\lambda^\epsilon \;=\; \frac{\int_{-\epsilon}^{\epsilon} d\cos\theta_L \; I_2^\lambda(\theta_L)}{\int_{-\epsilon}^{\epsilon} d\cos\theta_L \; [I_0^L(\theta_L) + I_0^T(\theta_L)]} \;, \tag{33}$$

where $\bar{\sigma}_{ee}^{P,\epsilon}$ is the SM cross section restricted to the angular range $|\cos\theta_L| < \epsilon$, and α_λ^ϵ are angular weights for the *graviton* interference effect on the cross section. Note that, due to Lorentz invariance, one must find $\alpha_\lambda^1 = 0$. Keeping $\epsilon < 1$, on the other hand, will give rise in general to nonvanishing *graviton* contributions to the cross sections.

From Figure 2a, by choosing an angular cut equal to the zeros of the corresponding angular distribution (that is $\epsilon \simeq 0.66$), one can optimize the total *graviton* contribution. Correspondingly, one gets the following weights for the transverse and longitudinal graviton components : $\alpha_T \simeq 0.36$ and $\alpha_L \simeq 0.16$.

Applying a similar strategy to the $\sqrt{S} = 1$ TeV case (cf. Figure 2b), one has, for $m_H = 300$ GeV, $\epsilon \simeq 0.86$ with $\alpha_T \simeq 0.18$ and $\alpha_L \simeq 0.09$. For $m_H = 500$ GeV, one can selects the central range where the graviton distribution keeps negative values, and set $\epsilon \simeq 0.60$. Correspondingly, one has $\alpha_T \simeq 0.13$ and $\alpha_L \simeq 0.43$.

Hence, one in general expects that the graviton coefficients in Table 1 will contribute to the measured cross section with reduction factors of a few tens percent according to Eq. (32). At the same time, the graviscalar contribution, having the same flat distribution as the SM signal, will always contribute by the total relative amount Δ_0 to both the total and the cut cross section.

5 Gravity interference effects at $\mu^+\mu^-$ colliders

A cleaner framework where to study gravity interference effects on the Higgs boson pole is clearly given by a Higgs boson factory. Although presently challenging from a technological point of view, a $\mu^+\mu^-$ collider with c.o.m. energies around m_H is the natural place where to realize a Higgs boson factory [12].

One then should consider the gravity interference with the Higgs exchange diagram for the process

$$\mu^+\mu^- \to P\bar{P} \;, \tag{34}$$

with $P = t, W, Z$.

For unpolarized initial states, the cross section for the latter process, including interference contributions with the graviscalar and graviton exchange graphs, can be expressed near the Higgs pole as:

$$\frac{d\sigma^P}{d\cos\theta} \;=\; \frac{\bar{\sigma}^P}{2} \; \left\{1 + \Delta_0^P + \Delta_2^P \; (1 - 3\cos^2\theta)\right\} \;, \tag{35}$$

where

$$\bar{\sigma}^P \;=\; \frac{d_P}{8\pi s}\,\frac{G_F^2 m_\mu^2 m_P^4}{(s-m_H^2)^2+m_H^2\Gamma_h^2}\,\sqrt{\frac{s-4m_P^2}{s-4m_\mu^2}}\,(s-4m_\mu^2)\,\rho_P\left(\frac{s}{m_P^2}\right)\,, \qquad (36)$$

with

$$\rho_t(x)=(x-4)\,,\qquad \rho_{W,Z}(x)=\frac{1}{2}(x^2-4x+12)\,, \qquad (37)$$

is the SM total cross section for the process in Eq. (34). Here, $\sqrt{s}$ is the total collision energy in the $\mu^+\mu^-$ c.o.m. frame, and the coefficients d_P for the different final states have the following values: $d_t=3$, $d_W=1$ and $d_Z=\frac{1}{2}$.

The coefficients Δ_0^P are the same as in Eq. (17)

$$\Delta_0^P = R_\delta\, c_P\left(\frac{\delta-1}{\delta+2}\right)\,, \qquad (38)$$

with $c_t=c_W=\frac{4}{3}$ and $c_Z=\frac{2}{3}$, and R_δ as in Eq. (17). For the coefficients Δ_2^P , one has instead

$$\Delta_2^t=-\frac{4}{3}\,R_\delta\,,\qquad \Delta_2^{W,Z}=R_\delta\,\frac{2}{3}\,\frac{(x-4)(x+6)}{x^2-4x+12}\,, \qquad (39)$$

with $x=s/m_{W,Z}^2$.

Note that $\Delta_2^{t,W}=\Delta_{2,T}^{t,W}$, with coefficients $\Delta_{2,T}^{t,W}$ defined as in Eq. (17). As a consequence of the above identities, a few numerical interesting values of $\Delta_0^{t,W}$ and $\Delta_2^{t,W}$, for $M_D=1$ TeV and $\delta=2$, can be found back in the Tables 1 and 2.

Even in the process $\mu^+\mu^-\to P\bar{P}$ the gravity interference effects can be quite large for high Higgs boson masses. Also in this case, in order to enhance the *graviton* contribution (that vanishes in the total cross section) it would be sufficient to properly exclude in the measured cross-section the forward-backward direction. This can be straightforwardly done in this case by properly cutting the θ range in Eq. (34).

6 Conclusions

In this paper, we computed gravity interference effects in Higgs boson production at future colliders in the framework of the models based on large compact extra dimensions proposed in [1]. In particular, we considered the Higgs production channel via WW fusion at linear colliders (that we treat in the effective W approximation) with a subsequent Higgs decay into pairs of heavy particles ($WW, ZZ, t\bar{t}$). We also analyzed Higgs production and decay channels at $\mu^+\mu^-$ Higgs factories. The interference of graviton/graviscalar exchange diagrams with *resonant* Higgs production and decay channels has the advantage with respect to usual virtual graviton/graviscalar

exchange channels to lead to a completely predictive determination in terms of the Planck scale M_D and number of extra dimensions δ. The effect on the SM angular distribution in general increases with the Higgs boson mass (for $\delta = 2$, the effect is proportional to $m_H\Gamma_H$). The *graviscalar* interference, that does not alter the shape of the distributions, changes its normalization by a few percent for $m_H > 500$ GeV, if $M_D \simeq 1$ TeV and $\delta = 2$.

On the other hand, due to the different spin properties of the *graviton* and Higgs boson amplitude, the graviton interference alters the angular shape by a universal $(1 - 3\cos^2\theta)$ distribution (in the W^+W^- or $\mu^+\mu^-$ c.o.m. frame) with a coefficient that is again of the order of a few percent for $m_H > 500$ GeV. The latter distribution is averaged to zero in the total cross section. Hence, in order to select a graviton effect, we suggest angular-cut strategies that enhance the *graviton* interference contribution in the measured cross section.

In order to detect such indirect graviton effects in Higgs cross section measurements, it is crucial that the actual experimental set up will be able to reach the required sensitivity. While assessing the final precision of muon colliders is premature at the moment, quite a few studies on this subject have been carried out for the linear e^+e^- colliders [9]. In particular, the precision expected on the measurement of the cross section for Higgs boson production via WW fusion has been considered in [14] (see also [15]) for a light Higgs decaying predominantly into b quark pairs, and is of the order of a few percent. A detailed study for heavier Higgs bosons (that are the relevant ones for our study) is presently missing, to our knowledge. Anyhow, a percent precision in the cross section measurements should allow to detect some effect at least in the most favorable case of $M_D \simeq 1$ TeV and $\delta = 2$ at both linear colliders and Higgs factories. The effect scales as $\sim 1/M_D^{2+\delta}$ with the Planck mass scale.

A complete treatment (i.e., beyond the effective W approximation) of the cross-section in the WW fusion process at linear colliders is not expected to alter our conclusions.

Note that, by the time experiments at linear colliders should be operating, the LHC will have presumably observed the direct production of gravitons in the range of parameters that could be relevant for our *precision* measurements. In particular, a direct graviton signal is expected, for $\delta = 2, 3, 4$, for M_D up to a few TeV's [16, 17]. The information derived from the direct graviton production and observation at LHC will definitely help in disentangling the deviations in the Higgs cross sections and distributions analyzed in the present paper.

Acknowledgments

We would like to thank M. Giovannini, M. Porrati, and M. Testa for useful discussions. E.G. and A.D. would also like to thank the Physics Department of University of Roma "La Sapienza", while E.G. thanks also the CERN Theory Division, for their kind of hospitality during the preparation of this work. A.D. and E.G. also thank Academy of Finland (project number 48787) for financial support.

References

[1] N. Arkani-Hamed, S. Dimopoulos and G. Dvali, Phys. Lett. **B429** (1998) 263 ; I. Antoniadis, N. Arkani-Hamed, S. Dimopoulos, and G. Dvali, Phys. Lett. **B436** (1998) 257.

[2] S. Dimopoulos and G. F. Giudice, Phys. Lett. B379 (1996) 105 ; J.C. Long, H. W. Chan and J. C. Price, Nucl.Phys.B539:23-34,1999.

[3] G. F. Giudice, R. Rattazzi and J. D. Wells, Nucl. Phys. B **544** (1999) 3.

[4] E. A. Mirabelli, M. Perelstein and M. E. Peskin, Phys. Rev. Lett. **82** (1999) 2236 .

[5] T. Han, J. D. Lykken and R. Zhang, Phys. Rev. D **59** (1999) 105006 .

[6] N. Arkani-Hamed, S. Dimopoulos and G. Dvali, Phys. Rev. D **59** (1999) 086004; J. L. Hewett, Phys. Rev. Lett. **82** (1999) 4765; C. Balázs, H.-J. He, W. W. Repko and C.-P. Yuan, Phys. Rev. Lett. **83** (1999) 2112; E. Dudas and J. Mourad, Nucl. Phys. B **575** (2000) 3; E. Accomando, I. Antoniadis and K. Benakli, Nucl. Phys. B **579** (2000) 3; S. Cullen, M. Perelstein and M. E. Peskin, Phys. Rev. D **62** (2000) 055012; W. D. Goldberger and M. B. Wise, Phys. Lett. **B475** (2000) 275; B. Grzadkowski and J.F. Gunion, Phys. Lett. **B473** (2000) 50; G. F. Giudice, R. Rattazzi and J. D. Wells, Nucl. Phys. B **630** (2002) 293; Nucl. Phys. B **595** (2001) 250; H. Davoudiasl, J. L. Hewett and T. G. Rizzo, Phys. Rev. Lett. **84** (2000) 2080; Phys. Lett. **B473** (2000) 43; Phys. Rev. **D63** (2001) 075004; T. G. Rizzo, Phys. Rev. **D64** (2001) 095010; E. Gabrielli and B. Mele, Nucl. Phys. B **647** (2002) 319; J. Hewett, M. Spiropulu, Ann. Rev. Nucl. Part. Sci. **52** (2002) 397; E. Dvergsnes, P. Osland and N. Ozturk, hep-ph/0207221; T. G. Rizzo, eConf

C010630 (2001) P301, hep-ph/0108235; M. Cavagliá, hep-ph/0210296; T. G. Rizzo, JHEP **0302** (2003) 008; G. C. Nayak, hep-ph/0211395; G. F. Giudice, A. Strumia, hep-ph/0301232; N. G. Deshpande, D. K. Ghosh, hep-ph/0301272.

[7] G. Landsberg, arXiv:hep-ex/0105039, and references therein.

[8] A. Datta, E. Gabrielli and B. Mele, Phys. Lett. B **552** (2003) 237.

[9] J. A. Aguilar-Saavedra *et al.* [ECFA/DESY LC Physics Working Group Collaboration], 'TESLA Technical Design Report Part III: Physics at an e+e- Linear Collider, hep-ph/0106315.

[10] See, for instance, M. Spira and P. M. Zerwas, hep-ph/9803257 .

[11] S. Dawson, Nucl. Phys. B **249** (1985) 42.

[12] see, e.g., HIGGS FACTORY 2001 SNOWMASS REPORT, http://www.physics.ucla.edu/hep/hfactory/index.html

[13] K. Hagiwara et al., Phys. Rev. **D66** 010001 (2002), http://pdg.lbl.gov/ .

[14] K. Desch and N. Meyer, LC-PHSM-2001-025 *In *2nd ECFA/DESY Study 1998-2001* 1694-1704.*

[15] S. Dawson and S. Heinemeyer, Phys. Rev. D **66** (2002) 055002.

[16] L. Vacavant and I. Hinchliffe, J. Phys. G **27** (2001) 1839.

[17] L. Vacavant, "Search for extra dimensions at LHC", talk given at the International Europhysics Conference on High Energy Physics EPS, July 17th-23rd, 2003, Aachen, Germany.